CLM - R 159

CLM - R 159

UKAEA RESEARCH GROUP

Report

COMPUTATIONS OF HYDROGEN ION SPECIES PRODUCED IN HIGH CURRENT ION SOURCES

A R MARTIN
T S GREEN

CULHAM LABORATORY
Abingdon Oxfordshire

1976
Available from H. M. Stationery Office

C 18

£1.50

UDC: 537.534.2:546.11

CLM-R 159

COMPUTATIONS OF HYDROGEN ION SPECIES PRODUCED IN HIGH CURRENT ION SOURCES

A R Martin and T S Green

(Euratom-UKAEA Fusion Association)

Culham Laboratory, Abingdon, OXFORDSHIRE OX14 3DB, UK

ABSTRACT

One requirement for high current ion sources for use in plasma physics research is the production of beams of ions with high proton fractions, similar to those obtained in low current sources used in nuclear physics applications. As a step towards the realisation of this requirement computations have been made of the competing processes occurring in a hydrogen plasma which determine the ratio of ion species. Results have been obtained for the case of a duoplasmatron and compared with published experimental data.

May 1976

SBN: 85311 046 8

1. INTRODUCTION

High current ion sources are at present being developed for application to neutral injection into large fusion experimental facilities[1,2,3]. One of the requirements[4] placed on these sources is that they should produce beams with fractions of H_1^+ ions $\gtrsim$ 80%, higher than those obtained with present sources[5,6].

Such high fractions have been obtained using duoplasmatrons[7,8] and R.F. sources[9] utilised in accelerators for nuclear physics studies. The factors which determine the yields of the different hydrogen ion species have been studied experimentally for both of these sources[7,8,9]. The interpretation of the data has been discussed initially by Thonemann[10] and more fully by Gabovich[11] and Goodyear and von Engel[12]. These discussions are limited to consideration of the most dominant reactions and of the conditions under which the H_1^+ yields may be maximised.

In this paper, we present an extension to these treatments to the computation of the competing reaction rates within the source plasma which allows one to estimate the ratio of the densities of H_1^+, H_2^+ and H_3^+ ions under different operating conditions. In order to derive results which may be applicable to different types of source, a two component electron energy distribution is utilised. One component is a high energy, mono-energetic, group corresponding to the primary current carrying electrons which are commonly assumed to be responsible for ionisation in duoplasmatrons[13,14] and reflex arc sources[15]. The other component is the thermal electron group assumed to have a Maxwellian energy distribution characterised by a temperature T_e.

The equations which relate the production and loss rates of neutral particles and of ions are discussed in section 2. They are similar to those discussed by Riviere et al[16] in analysis of the equilibrium composition of a hydrogen plasma in the Levitron experiment (in which case only thermal electrons are considered). An important difference is the equations for conservation of particles as discussed later. The cross-sections and the methods of computing reaction rates required for the solution of these equations are discussed in the Appendix.

From the equations it is possible to make a number of general predictions concerning the ratios of the neutral species and the ion species, as discussed in section 2.6. In order to demonstrate the applicability of the analysis to a particular problem, comparison is made of the computational results with the experimental data presented by Watanabe[8] for a duoplasmatron. This case is chosen because it is well documented and because it is a relatively simple type of source to analyse.

2. THE PARTICLE BALANCE EQUATIONS

2.1 Composition of the Partially Ionised Plasma

The partially ionised plasma consists of electrons, H_o atoms, H_2 molecules, H_1^+ ions, H_2^+ and H_3^+ molecular ions. The densities of the particles are specified, respectively, as n_e, N_1, N_2, n_1, n_2, and n_3. In this analysis it is assumed that the total density of the neutral particles is a constant, Q , i.e.

$$N_2 + \frac{N_1}{2} = Q \qquad (1)$$

being unaffected by the increase in n_e . Consequently the results

apply to the condition that the partial density of the neutral particles is Q_o, independent of the density of charged particles.

2.2 Reactions Occurring in the Plasma

The dominant reactions which occur between the species in the plasma are listed below, together with the symbols used to designate the average reaction rate coefficients for them.

Ionisation of atom	$H_o + e \rightarrow H_1^+ + 2e$	$\langle\sigma v\rangle_{11}$
Ionisation of molecule	$H_2 + e \rightarrow H_2^+ + 2e$	$\langle\sigma v\rangle_{21}$
Dissociation of molecule	$H_2 + e \rightarrow H_o + H_o + e$	$\langle\sigma v\rangle_{22}$
Dissociative excitation	$H_2^+ + e \rightarrow H_1^+ + H_o + e$	$\langle\sigma v\rangle_{23}$
H_3^+ formation	$H_2^+ + H_2 \rightarrow H_3^+ + H_o$	$\langle\sigma_x v_+\rangle$
Dissociation of H_3^+ ions	$H_3^+ + e \rightarrow H_2^+ + H_o + e$	$\langle\sigma v\rangle_{31}$.

Reactions which are neglected, either because of their low cross-section or because of insufficient data, are:-

$$H_2 + e \rightarrow H_1^+ + H_o + 2e$$

$$H_o + e \rightarrow H_o^* + e$$

$$H_o^* + e \rightarrow H_1^+ + 2e$$

$$H_2^+ + e \rightarrow H_1^+ + H_1^+ + 2e$$

$$H_2^+ + e \rightarrow H_o + H_o$$

and other channels for $H_3^+ + e$ break-up.

2.3 Loss Rate of Particles from the Plasma

The balance equations must allow for the loss of particles from the plasma to the walls. The rate of loss per unit volume is given by the density of the species divided by the containment time, when the particles recombine on the walls. It is assumed that all the species

of ions recombine at the wall to produce molecules.

However, in general, the H_o atoms only partially recombine: designating γ as the recombination factor for atoms, then the loss rate of the atoms equals $\gamma \frac{N_1}{T_1}$ where T_1 is the containment time of the atoms. T_1 is calculated from the expression

$$T_1 = \frac{4\ V.}{v_o\ A} \qquad (2)$$

where V is the source volume, A the surface area of the walls of the source and v_o the mean velocity of the H_o atoms. When the atoms are formed by dissociation of molecules or molecular ions they will have mean velocities greater than that of the molecules. However if the atoms have a low recombination factor on the walls, and a high thermal accommodation coefficient, they will be slowed down rapidly by wall collisions and the mean velocity will fall. This effect is neglected in the calculations presented below but will be considered in a more detailed discussion, of the effects of recombination on the species ratio, later.

The containment times of the H_1^+, H_2^+ and H_3^+ ions are designated as τ_1, τ_2 and τ_3 respectively. Their values will depend on the mechanisms which determine particle losses in the sources and must therefore be discussed in respect of each source under consideration.

2.4 Particle Balance Equations

We can now list the equations for the balance in production and loss for each species of neutral particle and ion as follows:-

(a) H_o

$$2N_2\ n_e\ \langle\sigma v\rangle_{22} + n_2\ n_e\ \langle\sigma v\rangle_{23} = N_1\ n_e\ \langle\sigma v\rangle_{11} + \frac{N_1}{T_1}\ \gamma \qquad (3)$$

(b) H_1^+

$$n_2\, n_e\, \langle\sigma v\rangle_{23} + N_1\, n_e\, \langle\sigma v\rangle_{11} = \frac{n_1}{\tau_1} \qquad (4)$$

(c) H_2^+

$$N_2\, n_e\, \langle\sigma v\rangle_{21} + n_3\, n_e\, \langle\sigma v\rangle_{31}$$

$$= n_2\, n_e\, \langle\sigma v\rangle_{23} + n_2\, N_2\, \langle\sigma_x v_+\rangle + \frac{n_2}{\tau_2} \qquad (5)$$

(d) H_3^+

$$n_2\, N_2\, \langle\sigma_x v_+\rangle = \frac{n_3}{\tau_3} + n_3\, n_e\, \langle\sigma v\rangle_{31} \,. \qquad (6)$$

2.5 Boundary Conditions

Equations 1 and 3-6 are a set of simultaneous equations relating the densities of neutrals, ions and electrons in which the coefficients are functions of the energy spectrum of the ionising electrons. However, they do not give a complete description of the particle balance in the plasma; to obtain this one must add a boundary condition which interrelates the electron density to the electron energy spectrum.

The simplest example of such a boundary condition is that in a plasma in which the ionisation is produced by thermal electrons, n_e is the density of the thermal electrons which are characterised by a temperature T_e . One must now specify, as a boundary condition, that the electron density should equal the total ion density

i.e. $$n_e = n_1 + n_2 + n_3 \,. \qquad (7)$$

In this case it can be shown that there is only one value of the electron temperature for which the equations are satisfied at a specified value of Q, T_1, τ_1, τ_2 and τ_3 [16].

This result is a generalisation of that obtained in discussion of

RF sources[17] and P.I.G. sources[18], in which the balance between the rate of production of ions and the rate of loss has been calculated, in a monatomic gas e.g.

$$n_o \, n_e \, \langle \sigma v \rangle_{ION} = \frac{n_+}{\tau_+}$$

and

$$n_e = n_+ \quad .$$

Hence

$$\langle \sigma v \rangle_{ION} = \frac{1}{n_o \, \tau_+} \quad ,$$

where n_o is the neutral gas density, $\langle \sigma v \rangle_{ION}$ the rate coefficient for ionisation which is a function of temperature, and n_+, n_e, τ_+ are defined as above. Thus for a given value of n_o and τ_+ there is only one consistent value of $\langle \sigma v \rangle_{ION}$ and only one possible value for the electron temperature.

Another limiting case is that in which the ionising electrons are mono-energetic current carrying electrons so that

$$n_e < n_1 + n_2 + n_3 \quad .$$

The boundary condition which should now be imposed is the Langmuir sheath stability criterion which relates the electron current I_e to the ion current to the cathode I_{+c}[13,14,19] (or to the double sheath in duoplasmatrons)

$$I_e = \alpha \sqrt{\frac{m_i}{m_e}} \; I_{+c} \qquad (8)$$

where m_i, m_e are the ion and electron masses respectively and α is a constant of order unity. In order to utilise this boundary condition it is necessary to relate I_e to n_e and I_{+c} to the total ion production rate. The relation between I_{+c} and the total ion production rate

depends on geometrical factors and on the influence of magnetic fields[20]. In general, therefore, it is a complicated relation, although in a few cases one may use approximations to obtain results (e.g. the duoplasmatron[13,14] and magnetic field free sources[21]).

The relation between I_e and n_e is derived from analysis of the balance of input and loss mechanisms for the ionising electrons[22]. It may be written, at least for magnetic field free sources, in the form,

$$\frac{I_e}{eV} = \frac{n_e}{\tau_e} + n_e N_1 \langle \sigma v \rangle_{IN.1} + n_e N_2 \langle \sigma v \rangle_{IN.2} \qquad (9)$$

where $\langle \sigma v \rangle_{IN.1}$ is the rate coefficient for inelastic scattering of the electrons by atomic hydrogen, $\langle \sigma v \rangle_{IN.2}$ that for inelastic scattering by molecular hydrogen, and τ_e the electron containment time.

The complexity of these two relations makes it difficult to utilise the boundary conditions (equation 8), in order to provide a complete description of the source plasma, at least at the present. Consequently, in the present analysis, we treat n_e as a free parameter and calculate the particle densities as a function of n_e. We will consider the relationship between n_e and the electron current, in a future communication.

2.6 General Remarks Concerning Solutions

2.6.1 H_2^+/H_2 ratio

To a first approximation the ratio of H_2^+/H_2 densities, i.e n_2/N_2, is a measure of the degree of ionisation in the source. From the balance equations, one derives the result

$$\frac{n_2}{N_2} = \frac{\langle \sigma v \rangle_{21}}{\langle \sigma v \rangle_{23} + \frac{1}{n_e \tau_2}} \quad . \qquad (10)$$

Thus one can calculate n_2/N_2 as a function of $n_e \tau_2$ for different assumed energy spectra, as shown in fig. (1). The data show that

$\frac{n_2}{N_2}$ tends to a limit at high values of $n_e \tau_2$. It follows from equation (10) that this limit is $\frac{\langle\sigma v\rangle_{21}}{\langle\sigma v\rangle_{23}}$ which has a value of $\sim$ 0.1-0.4 depending on the electron energy. The limit is reached when $n_e \tau_2 >> \langle\sigma v\rangle_{23}^{-1} \sim 6 \times 10^6 - 2 \times 10^7$ sec cm^{-3}.

It should be noted however that there is a fundamental limit to the attainable value of $n_e \tau$ in ion sources due to the phenomenon of arc starvation, i.e. the depletion of neutral density in the source by ionisation [14,21]. Calculations of the influence of starvation on the operation of sources depend in detail upon the boundary conditions applying to particle balance as outlined above. However, one may make a general statement that arc starvation becomes a limiting influence on operation when the mean free time for a neutral to be ionised is less than the mean flight time of neutrals across the source, T_2, i.e. when

$$n_e \langle\sigma v\rangle_{21} T_2 \sim 1 \quad .$$

Thus arc starvation limits n_e to such a value that

$$n_e \tau \simeq \frac{\tau}{T_2} \cdot \frac{1}{\langle\sigma v\rangle_{21}} \quad .$$

For the case in which mono-energetic electrons dominate, this limit is $\sim \frac{\tau}{T_2} \times 2.0 \times 10^7$ sec cm^{-3}, whilst for a thermal plasma ($T_e \sim 10$ eV) it is $\frac{\tau}{T_2} \times 1.25 \times 10^8$ sec cm^{-3}. Unless the ions are magnetically confined $\tau << T_2$; typically τ/T_2 equals the square root of the ratio of the thermal energy of the neutral ($\sim$ 1/40 eV) to the thermal energy of the ion ($\sim$ 1 eV) i.e. 0.16. Thus the limiting values of $n_e \tau$ may be 3×10^6 sec cm^{-3} for mono-energetic electrons, and 2×10^7 sec cm^{-3} for thermal electrons.

This restriction on $n_e \tau$ implies that it is not possible to reach the high electron density limit for n_2/N_2 .

2.6.2 H_3^+/H_2^+

The ratio of densities of the H_3^+ and H_2^+ ions is given by the expression

$$\frac{n_3}{n_2} = \frac{N_2 \langle \sigma_x v_+ \rangle}{\frac{1}{\tau_3} + n_e \langle \sigma v \rangle_{31}} \qquad (11)$$

or

$$\frac{n_3}{n_2} = . \frac{1}{1 + n_e \tau_3 \langle \sigma v \rangle_{31}} \times \frac{\tau_3}{\tau_x} \qquad (11a)$$

where τ_x is the mean free time for charge exchange leading to H_3^+ production. At low electron densities n_3/n_2 equals $\frac{\tau_3}{\tau_x}$. At higher densities the density of H_3^+ is depleted by electron dissociation of the ion at a rate which depends on the electron energy spectrum - though not too sensitively (fig. 2).

As discussed in the previous section $n_e \tau$ is limited by the onset of arc starvation. Limiting discussions to the case of mono-energetic electrons, $n_e \tau$ is less than 3×10^6 sec cm^{-3}. Since $\langle \sigma v \rangle_{31}$ is $\sim 1.5 \times 10^{-7} cm^3 sec^{-1}$ for such electrons (fig.A4), $n_e \tau_3 \langle \sigma v \rangle_{31}$ is unlikely to rise above a value of ~ 0.5.

One can therefore consider that reduction of the H_3^+ density by electron dissociation of the ion is unlikely to become a dominant process in ion sources, and that the only method of producing low yields of H_3^+ is to operate with low neutral molecule number densities.

2.6.3 H^+/H_2^+

The ratio of the densities of H^+ and H_2^+ ions is given by the expression

$$\frac{n_1}{n_2} = n_e \tau_1 \langle\sigma v\rangle_{23} \left[1 + \frac{\left\{ 1 + 2 \frac{\langle\sigma v\rangle_{22}}{\langle\sigma v\rangle_{21}} \left(1 + \frac{1}{n_e \tau_2 \langle\sigma v\rangle_{23}} \right) \right\}}{1 + \frac{\gamma}{n_e T_1 \langle\sigma v\rangle_{11}}} \right] \quad (12)$$

The first term in this bracket derives directly from the dissociative ionisation of H_2^+ molecular ions; the second term derives from ionisation of H_o atoms which are in turn produced either by dissociative ionisation of the H_2^+ molecular ions or by dissociation of the H_2 molecule. One problem in evaluating this ratio arises from the fact that the reaction rate for dissociation of the molecule ($\langle\sigma v\rangle_{22}$) peaks strongly at low energies (figure A3): thus this term is much more sensitive to the energy spectrum than any other term.

There are two limiting approximations for equation 12. At low $n_e \tau_2$ values one has

$$\frac{n_1}{n_2} \simeq n_e \tau_1 \langle\sigma v\rangle_{23} \left[1 + \frac{2 \langle\sigma v\rangle_{11}}{\langle\sigma v\rangle_{23}} \cdot \frac{\langle\sigma v\rangle_{22}}{\langle\sigma v\rangle_{21}} \frac{T_1}{\gamma \tau_2} \right] \quad (12a)$$

i.e. $\frac{n_1}{n_2}$ is proportional to n_e .

At high values of $n_e \tau$ one finds

$$\frac{n_1}{n_2} \approx 2 n_e \tau_1 \langle\sigma v\rangle_{23} \left[1 + \frac{\langle\sigma v\rangle_{22}}{\langle\sigma v\rangle_{21}} \right] . \quad (12b)$$

Again n_1/n_2 is proportional to n_e , although the proportionality factor is different.

The shape of the transition from one limit to the other depends sensitively on the reaction rate ratio $\frac{\langle\sigma v\rangle_{22}}{\langle\sigma v\rangle_{21}}$ and on the recombination factor. This point will be considered in a further communication.

3. COMPARISON OF NUMERICAL RESULTS WITH EXPERIMENTAL DATA FOR A DUOPLASMATRON

3.1 Experimental Data

An experimental study of the ratios of the currents of the different ion species extracted from a hydrogen plasma in a duoplasmatron has been reported by Watanabe[8].

The configuration of the source is shown in fig. 3. There are two plasma volumes, that between the cathode and intermediate electrode and that between the intermediate electrode and the anode. It is assumed that the ions, which are extracted, are produced in the latter volume, and that it is with the characteristics of the plasma in this volume that we are concerned[13,14].

The experimental data were obtained with the source operating in the arc current range 0.5 to 2.0 Amps and in the pressure range 0.05 - 0.4 torr. The influence of current and pressure on the ratios of the extracted currents of the different ion species is shown in figs. 4 and 6. Watanabe also investigated the influence of the magnetic field and the spacing of the intermediate electrode and the anode (figures 5, 7 and 8). In the following discussion it is assumed that the extracted current is proportional to the ion density divided by the ion containment time.

3.2 Source Parameters required for Calculations

In order to calculate the ratios of the extracted currents of the different species using equations 1-6 it is necessary to know the total neutral particle density, the electron density and energy spectrum,

the particle containment times T_1, τ_1, τ_2 and τ_3 and the wall recombination factor γ . The total neutral density Q is calculated from the gas pressure. The wall recombination factor is estimated from the data for recombination on the various components of the source[23], a value of γ equal to 0.1 being used.

The electron density and energy spectrum present a problem. Watanabe reports that there is a region of intense ionisation (the so-called fireball) in the intermediate electrode in which the electron temperature is 15 eV. However calculations performed, assuming that the thermal electrons have a temperature of this value, lead to excessive values of the total ion density and violation of the condition that the density of the thermal electrons should equal that of the ions. It has therefore been assumed that these electrons do not contribute significantly to the collisional processes in the ion production zone. Instead, it is assumed that the dominant electrons are the current carrying electrons which gain an energy of 40 eV, in being accelerated across the double sheath in the intermediate electrode. (The measured potential difference from cathode plasma to anode was 40 volts). Since these electrons make a single transit of the plasma volume to reach the anode, their "containment time" is very short and one may approximate equation (9) to the form

$$\frac{n_e \, eV}{\tau_e} = I_e$$

or

$$n_e \, A \, e \, v_e = I_e \quad , \tag{13}$$

since $\tau_e \simeq V/v_e A$.

There is some uncertainty in the exact value of the area, A , of the beam of electrons passing through the plasma; consequently we have chosen to use the ratio of n_e to I_e as a normalisation factor deter-

mined by analysis of the data for H_3^+ and H_2^+ as discussed below. This normalisation is then carried through the calculations.

The containment time of the H_o atoms, designated T_1, is given by equation 2. The value of $\frac{V}{A}$ is estimated from the dimensions of the source to be 0.2 cm: this value may be an over estimate due to over-estimation of the radius of the ionisation volume (see section 3.3 and 3.5 below). The value of v_o used for the neutrals is 2×10^6 cm sec^{-1} derived on the assumption given above that the H_o neutrals are created with energies of $\sim$ 1 eV. Using these values for V/A and v_o we derive a value of 0.4×10^{-6} secs for T_1 . As will be seen below T_1 and γ enter as a factor $\gamma \tau_2/T_1$ which can be chosen to give a best fit to the data.

The values of the ion containment times also present a problem in that there is no experimental data from which they can be derived, and there is no clearly defined model of particle containment from which they may be estimated. For the purposes of this calculation we have assumed that the ratio of τ_1, τ_2 and τ_3 is in the ratio of the square root of the ion masses i.e. $1 : 2^{\frac{1}{2}} : 3^{\frac{1}{2}}$. Following this, τ_2 has been derived from the data for the yield of H_3^+ as discussed below. This value has then been carried through all the calculations.

3.3 Variation of Species Ratios of H_2^+ and H_3^+

3.3.1 Dependence on Arc Current

The ratio of the currents of H_2^+ and H_3^+ ions, designated respectively as I_2 and I_3, is derived from equation 11:-

$$\frac{I_2}{I_3} = \frac{n_2}{\tau_2} \cdot \frac{\tau_3}{n_3} = \frac{1}{N_2 \langle \sigma_x v_+ \rangle \tau_2} \left[1 + n_e \langle \sigma v \rangle_{31} \tau_3 \right] . \qquad (14)$$

Since n_e is proportional to I_e, as discussed above one expects a linear variation of I_2/I_3 with arc current. The experimental data are in agreement with this prediction as shown in figure 9.

By fitting a straight line to the data one obtains an intercept of 0.29 and a slope of 0.075 A^{-1}. The intercept equals $\left[N_2 \langle\sigma_x v_+\rangle \tau_2\right]^{-1}$. Inserting the known values of N_2 and of $\langle\sigma_x v_+\rangle$ one derives an estimate for the value of the containment time τ_2 equal to 3.3×10^{-7} secs.

From the value of the slope and the known value of $\langle\sigma v\rangle_{31}$ one estimates the value of $n_e \tau_3$ at 1 Amp arc current to be 1.7×10^6 sec cm^{-3}. The corresponding value of $n_e \tau_2$ is 1.4×10^6 sec cm^{-3} (using the scaling law for τ_1, τ_2, τ_3 discussed above). It therefore follows that n_e is equal to 4.2×10^{12} cm^{-3} at 1 Amp arc current and that the radius of the current channel is 0.36 mm (from equation 13 assuming 40 eV electrons). This value is lower than one would expect from the geometry, but the discrepancy is not serious.

3.3.2 Dependence on Pressure

Equation 14 also predicts that the ratio of I_3/I_2 should vary linearly with gas pressure in the source, provided that the particle containment times are independent of pressure, i.e. that they are not determined by diffusion processes. The plot of experimental data for I_3/I_2 versus pressure show a linear variation except at the highest pressures (fig. 10). This may be taken as an indication that diffusion only plays a significant role at these highest pressures.

On the other hand, the containment times derived may be compared with values predicted either assuming that the ions move without collisions (free-fall model[24]) or that they diffuse axially with

a velocity determined by the mobility.

The containment time of the H_2^+ ions derived above, (3.3×10^{-7} secs) corresponds to an escape velocity of 3×10^5 cm sec^{-1}. This velocity is somewhat lower than one would expect from the free fall model. This model predicts a value of $\sim \sqrt{\frac{k T_e}{m_i}}$ which is only in agreement with the experimental value if the temperature has the rather low value of 0.1 eV.

Values of the drift velocities of molecular ions in molecular hydrogen vary with the E/p values[25]. The derived velocity of 3.0×10^5 cm sec^{-1} is consistent with an E/p value of 30 volts/cm torr. At the operating pressure of 0.26 torr, this corresponds to an electric field of 7.8 volts/cm, which implies a rather low temperature ($\sim$ 1 eV) plasma of $\sim$ 2 mm length.

Thus both models lead to similar conclusions concerning the plasma conditions required to explain the observed escape velocity, and one cannot discriminate between them on this basis.

3.4 Variation of Species Ratios with Arc Current, $H^+ : H_2^+$

The ratio of the currents of H^+ and H_2^+ ions (designated I_1 and I_2) may also be calculated from the particle balance equations (equation 12)

$$\frac{I_1}{I_2} = n_e \tau_2 \langle\sigma v\rangle_{23} \left[1 + \frac{\left\{ 1 + \frac{2 \langle\sigma v\rangle_{22}}{\langle\sigma v\rangle_{21}} \left(1 + \frac{1}{n_e \tau_2 \langle\sigma v\rangle_{23}} \right) \right\}}{1 + \frac{\gamma}{n_e T_1 \langle\sigma v\rangle_{11}}} \right] . \quad (15)$$

As discussed in section 2.6.3 above, the difficulty in utilising this equation arises from uncertainties in the ratio $\langle\sigma v\rangle_{22}/\langle\sigma v\rangle_{21}$ which can take values from 0.26 for mono-energetic 40 eV electrons to 2.2 for mono-energetic 20 eV electrons reaching a value of 6.7 for

thermal electrons of 4 eV temperature. Consequently a reasonable admixture of lower energy and thermal electrons to the dominantly 40 eV primary group can increase $\langle\sigma v\rangle_{22}/\langle\sigma v\rangle_{21}$ from the value of 0.26 to a value of 1 or 2.

In order to derive an estimate of the value of $\langle\sigma v\rangle_{22}/\langle\sigma v\rangle_{21}$ which gives a best fit to the data, we have plotted the experimental data in the form I_1/I_2 versus I_e as shown in figure 11, and calculated the dependence to be expected, using the normalisation for converting $n_e \tau_2$ to I_e determined in the previous section, for a range of values of $\langle\sigma v\rangle_{22}/\langle\sigma v\rangle_{21}$ and the parameter $\frac{\gamma \tau_2}{T_1}$. Agreement can be obtained up to 1.2 Amps current for a reasonable set of values. However the high value of I_1/I_2 at 1.6 Amps can only be explained using a somewhat excessive value of $\langle\sigma v\rangle_{22}/\langle\sigma v\rangle_{21}$ equal to 3.0. It seems unwise to conclude that there is a real discrepancy here, in view of the limited number of experimental data points.

3.5 Computations of Species Fractions

In the previous two sections we have analysed the data for variation of the current ratio I_2/I_3 with arc current and pressure and of the ratio I_1/I_2 with current. Using the normalisation factors so obtained we have calculated the current fractions I_1/I_T , I_2/I_T and I_3/I_T (I_T is the sum of I_1, I_2 and I_3) and have shown them in figures 4 and 6 compared with the experimental data for completeness.

In the following sections we utilise these normalisation factors to calculate the variation of the current fractions with magnetic field and with electrode spacing.

3.6 Variation of Species Ratios with Magnetic Field

The experimental data show that the magnetic field strength in the source has a marked influence on the ratios of the species. To

understand this effect it is necessary to consider the influence of the magnetic field on the operation of the source. Lejeune[14] has proposed that the field controls the radius (a) of the current channel in the source so that 'a' varies inversely as the field strength B . Consequently the density of electrons in the beam, which is proportional to a^{-2}, varies as B^2.

We have calculated the variation of the species ratios with B on the assumption that n_e varies as B^2, all other parameters being constant (except T_1 the transit time of neutral atoms across the beam which varies as a and thus as B^{-1}). The result, shown in fig. 5b, agrees moderately well with the experimental data except at high values of the field strength.

This discrepancy may be explained on the reasonable assumption that the beam diameter cannot decrease indefinitely as B increases, due to the finite source dimensions. Thus we write

$$a = a_o \left(1 + \frac{B_o}{B}\right) \quad .$$

Clearly a wide range of fits can be obtained by varying a_o and B_o . Fig. 5c shows one example for the case a_o and B_o equal to 0.4 mm and 4 kG respectively.

3.7 Variation of Species Ratio with Electrode Spacing

Data obtained by Watanabe on the effect of changing the spacing D of the intermediate electrode and anode are shown in figures 7 and 8. Variation of the spacing produces changes in the species ratios essentially because the ion containment times vary. If the motion corresponded to the free fall model then one would expect linear scaling. However if the ions diffuse axially out of the plasma volume then the containment times would scale as the square of the spacing i.e.

as D^2. Calculations on the effect of changing D have been made using both scaling laws. The calculations based on the D^2 scaling give better agreement with the experimental data. This result suggests that ion loss is by diffusion in contradiction to the implication of the data in the previous section.

4. CONCLUSIONS

Detailed computations of the densities of the different ion species in a hydrogen plasma in an ion source can be made provided that one knows the cross-sections of the important collisional processes on the one hand, and the characteristics of the plasma and source on the other. In particular one needs to know the energy spectrum and density of the ionising electrons and the containment time of the ions.

At present the state of knowledge concerning these factors is not so advanced as that concerning the cross-sectional data. We have therefore chosen a relatively simple source system, i.e. the duoplasmatron, to test our computations and our assignment of the important collisional processes discussed in section 2.2.

The underlying assumption in our model of ionisation in the duoplasmatron is that the ionising electrons are mono-energetic, current carrying electrons, as proposed by Demirkhanov et al[13] and by Lejeune[14]. It follows from this assumption that the electron density is directly proportional to the arc current and inversely proportional to the cross-sectional area of the current channel, which in turn depends on the magnetic field. The computations of the variation of species ratio with current and magnetic field, based on these proportionalies, agree well with the experimental data and so substantiate the model.

The normalisation from electron density to arc current is consistent with the radius of the current channel being 0.36 mm.

This is much smaller than the radius of the aperture in the intermediate electrode (1.25 mm), as one would expect since the beam is focussed through the centre of the aperture; it is also slightly smaller than the radius of the aperture in the anode (0.4 mm) which one would not expect, since the electrons should be collected on the anode without crossing magnetic field lines.

The other normalisation required to fit the data is the assignment of an absolute value for the containment time of the H_2^+ ions. Although the value chosen is more consistent with the assumption that the ions diffuse axially out of the source, i.e. that τ_2 depends on the ion mobility, the scaling of species ratios with gas pressure indicate strongly that this is not the case. The complexity of the situation is underlined by the results of computations on scaling with electrode spacing, D , which suggest diffusion to be more important. However, in the geometry of this source it is not clear that the plasma column length is exactly the same as the electrode spacing, so that this result may be misleading. Finally, it should be noted that the mean free path for elastic ion-neutral collisions at the gas pressures involved is of the order of a millimetre i.e. one is working close to the boundary between the diffusion - dominated and free-fall regimes. Indeed the data for scaling of I_2/I_3 with gas pressure indicates a transition to the diffusion model at pressures above 0.3 torr.

The overall agreement between the computed ratios and the experimental data lead one to presume that the most important collisional processes have been taken into account and that the cross-sections assigned are reasonably accurate. The variation of the ratio of H_2^+

to H_1^+ with arc current can be accounted for by assuming a high cross-section for production of H_o from H_2 due to contributions from thermal electrons. An alternative explanation of this difference is that we have neglected the dissociative recombination reaction

$$H_2^+ + e \rightarrow H_o + H_o$$

which has a large cross-section at low electron energies[26]

$$\text{i.e.} \qquad \sim 10^{-15} \text{ cm}^2 \text{ at } \sim 1 \text{ eV} .$$

The general conclusions which can be drawn from this study for application to analysis of other sources are that the ratio of H_3^+ to H_2^+ is given to 20% accuracy by a modified form of equation 11 i.e.

$$\frac{n_3}{n_2} = N_2 \langle \sigma_x v_+ \rangle \tau_3$$

except at higher values of $n_e \tau_+$ than can be attained in many sources.

Similarly the ratio H_2^+ to H_2 is given by the approximate equation (valid to 20%)

$$\frac{n_2}{N_2} \simeq \langle \sigma v \rangle_{21} n_e \tau_2 .$$

These relationships indicate that the species ratio for sources can only be estimated if the values of n_e and ion containment times are known. This is certainly not generally the case. However, as discussed above in section 2.6.1, there is a limiting value for the product $n_e \tau_+$ set by the condition that the neutrals can penetrate the plasma, i.e. that one cannot exceed the arc starvation limit. It is a consequence of this limit that the ratio n_2/N_2 and n_1/n_2 have themselves got upper limits. Future experimental and theoretical work will be directed towards the evaluation of these limits.

APPENDIX

CROSS-SECTIONS AND RATE COEFFICIENTS

In section 2.2 six collisional processes were identified as being most important in determining the balance of the ion species in the source plasma. A discussion of the available information concerning these and competing reaction cross-sections has been presented by Martin[26].

The cross-section data allow us to ignore several reactions. Ionisation from excited states of the atom can be ignored because the cross-section for excitation to the 2S metastable state is much lower than the cross-section for ionisation, and the 2P radiative state has a short lifetime. Dissociative ionisation of H_2 to produce a proton and an atom has a cross-section over an order of magnitude smaller than that for ionisation to H_2^+. The dissociative ionisation cross-section of H_2^+ is also an order of magnitude lower than that for dissociative excitation.

The reactions for dissociative recombination of H_2^+ and breakup of H_3^+ to form neutral atoms, or to form protons, have also been neglected, as cross-sectional data have not been available for these reactions until recently. Recombination of H_2^+ is likely to play a role in the physics of the discharge as its cross-section is large at thermal electron energies, and the effect of this reaction should be taken into account in more detailed studies. The situation with H_3^+ breakup is still unsatisfactory, and no comprehensive data exist on the various reaction cross-sections.

The calculations of the reaction rates in the plasma require as input data rate coefficients, $\langle\sigma v\rangle$, which must be derived from the available cross-section data. The procedure adopted for determining

the rate coefficients followed closely that used by Freeman and Jones[27]. The values of σ were expressed as polynomial functions of velocity, the coefficients being chosen to fit the published experimental data, extended where necessary by Gryzinski calculations. From these polynomials it is a straightforward matter to compute the products σv for mono-energetic electrons and the values of $\langle \sigma v \rangle$ averaged over a Maxwellian distribution for thermal electrons.

Typical values of the reaction rate coefficients obtained in the above manner are shown in Figures A1-A4. The value of $\langle \sigma_x \, v_+ \rangle$ was taken to be constant, and equal to 1.5×10^{-9} cm^3 sec^{-1}.

REFERENCES

1. MORGAN, O.B., Paper VI-1, Proc. 2nd Symp. on Ion Sources and Formation of Ion Beams, LBL-3399 (1974).
2. THOMPSON, E., Paper VI-2, ibid.
3. SEMASHKO, N.N., Paper VI-3, ibid.
4. SHEFFIELD, J., Private communication.
5. COUPLAND, J.R. and THOMPSON, E., Paper VI-8, ibid Ref.1.
6. BERKNER, K.H. et al, Paper VI-12, ibid Ref. 1.
7. KELLEY, G.G., LAZAR, N.H. and MORGAN, O.B., Nucl. Instr. and Methods, 10, 263 (1961).
8. WATANABE, M., Jap. J. Appl. Phys., 6. 1127 (1967).
9. THONEMANN, P.C., MOFFAT, J., ROAF, D. and SANDERS, J.H., Proc. Phys. Soc., 61, 483 (1948).
10. THONEMANN, P.C., Prog. Nucl. Phys., 3, 219 (1953).
11. GABOVICH, M.D., "Physics and Engineering of Plasma Ion Sources", Moscow Atomizdat (1972). (translation FTD-HT-23-1690-72, Foreign Tech. Div. US Air Force).
12. GOODYEAR, C.C. and von ENGEL, A., p.203 in Proc. 5th Int. Conf. on Ionisation Phenomena in Gases, H. Maecker (Ed.), North Holland Pub. Co.
13. DEMIRKHANOV, R.A., FRÖHLICH, H., KURSANOV, V.V. AND GUTKIN, T.I., High Energy Accelerator Papers from USSR, BNL 767 (C-36), 1962.
14. LEJEUNE, C., p.27 in Symp. on Ion Sources and Formation of Ion Beams, BNL 50310 (1971).
15. GREEN, T.S., Paper I-2, ibid Ref. 1.
16. RIVIERE, A.C. and JONES, E.M. (to be published).
17. VON GOELER, S., p.399 in Proc. Int. Conf. Electromagnetic Isotope Separators, Marburg (BMBW-FB K70-28), H. Wagner and W. Walcher (Eds.) 1970.
18. GREEN, T.S. and GOBLE, C., Nucl. Ins. Meth., 116, 165 (1974).

19. BOHM, D., Chap. 4 in The Characteristics of Electric Discharges in Magnetic Fields, A. Guthrie and R.K. Wakerling (Eds.), McGraw-Hill, 1949.

20. BURHOP, E.H.S., MASSEY, H.S.W. and PAGE, G., Chap. 5, ibid Ref. 19.

21. GREEN, T.S., Bull. Am. Phys. Soc., 18, 1321 (1973).

22. GREEN, T.S., GOBLE, C., INMAN, M. and MARTIN, A.R., VIIth European Conf. on Cont. Fusion and Plasma Physics, 1975 (to be published).

23. WOOD, B.J. and WISE, H., p.51 in Proc. 2nd Int. Symp. on Rarefied Gas Dynamics, L. Talbot (Ed.), Academic Press, 1961.

24. TONKS, L. and LANGMUIR, I., Phys. Rev., 34, 876 (1929).

25. ROSE, D.J., J. Appl. Phys., 31, 643 (1960).

26. MARTIN, A.R., Culham Report CLM-R157 (1976).

27. FREEMAN, R.L. and JONES, E.M., Culham Report CLM-R137 (1974).

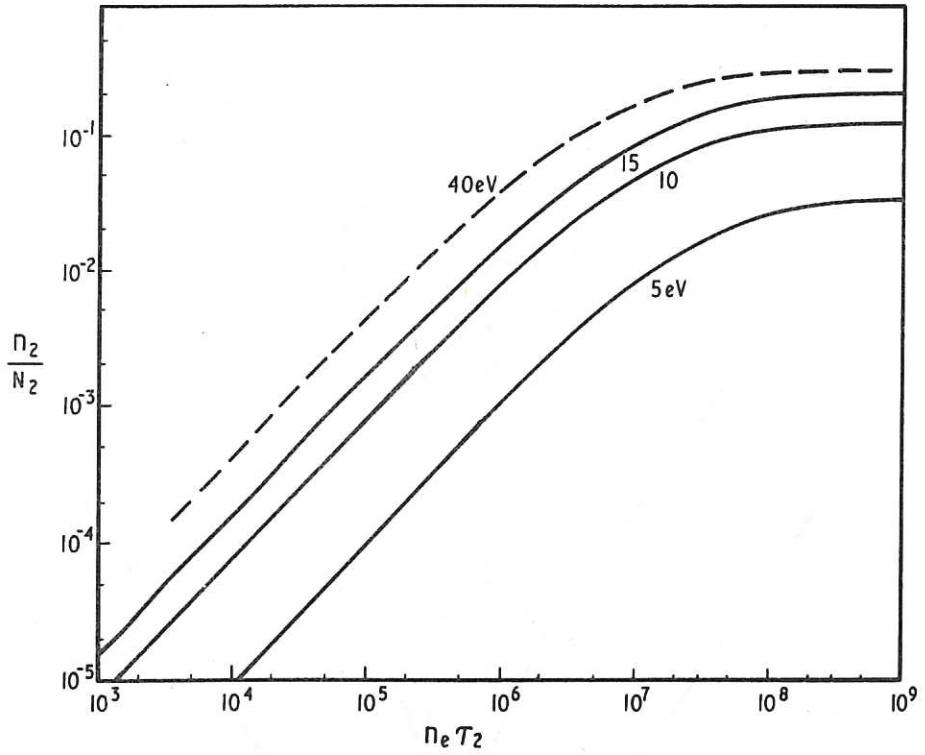

Fig.1 H_2^+/H_2 ratio as a function of $n_e\tau_2$. Solid lines – Maxwellian electrons only: Dashed line – 40eV monoenergetic electrons only.

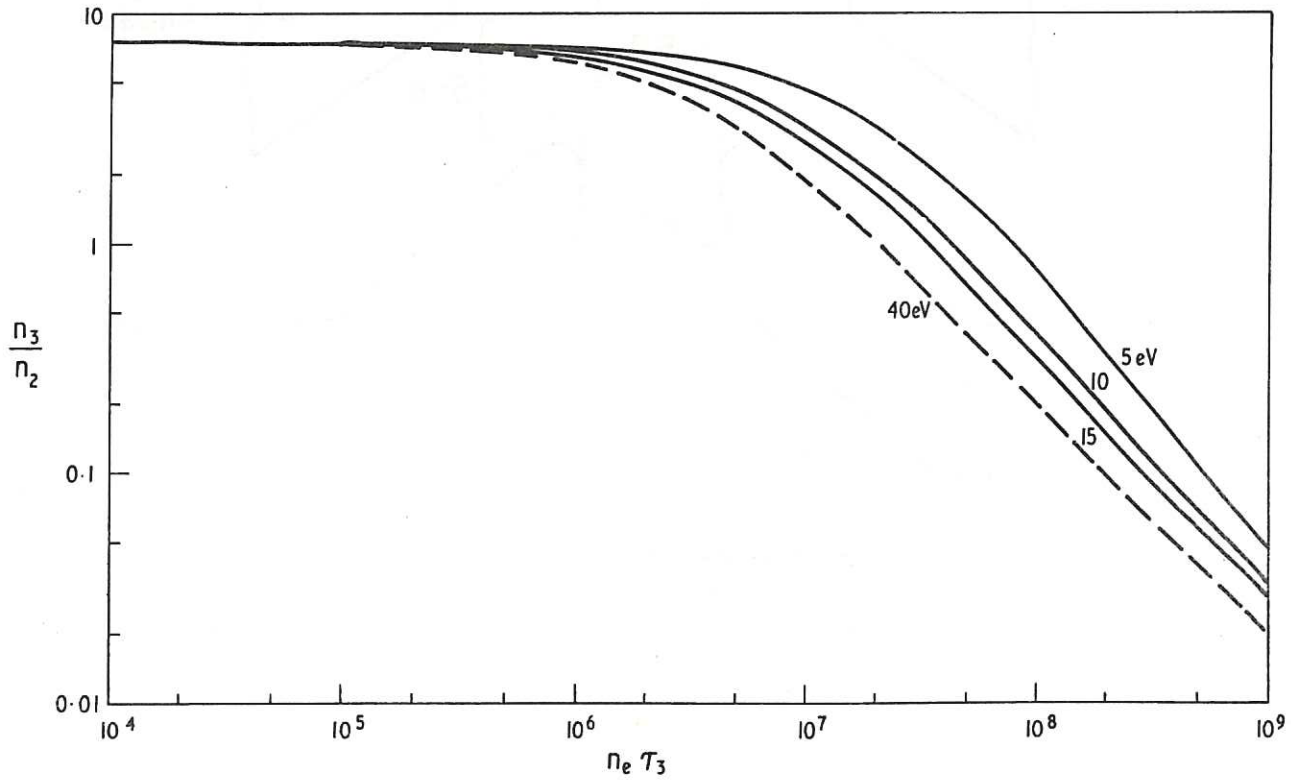

Fig.2 H_3^+/H_2^+ ratio as a function of $n_e\tau_3$. Solid lines – Maxwellian electrons only: Dashed line – 40eV monoenergetic electrons only.

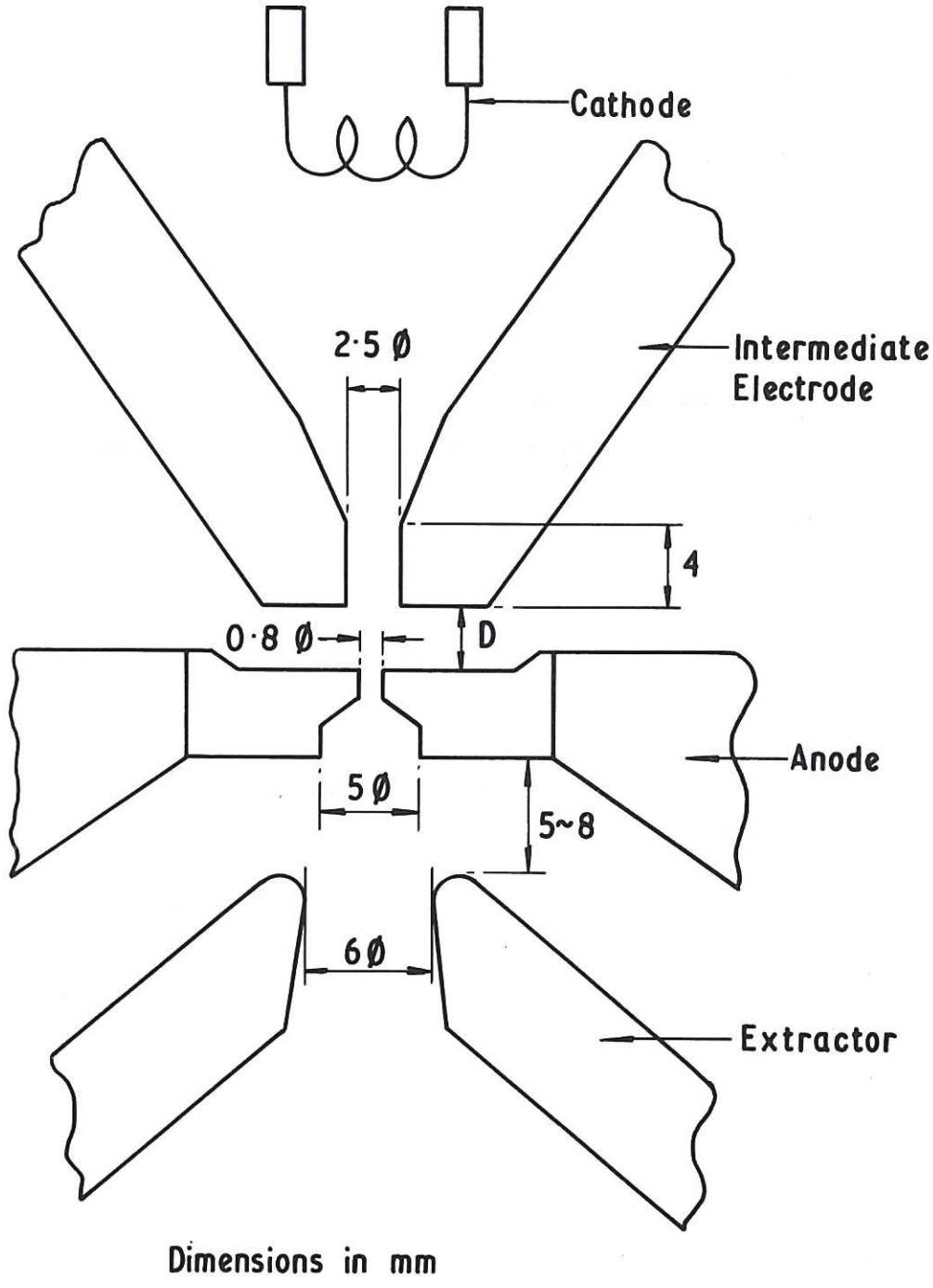

Fig.3 Diagram of the duoplasmatron source geometry used by Watanabe.

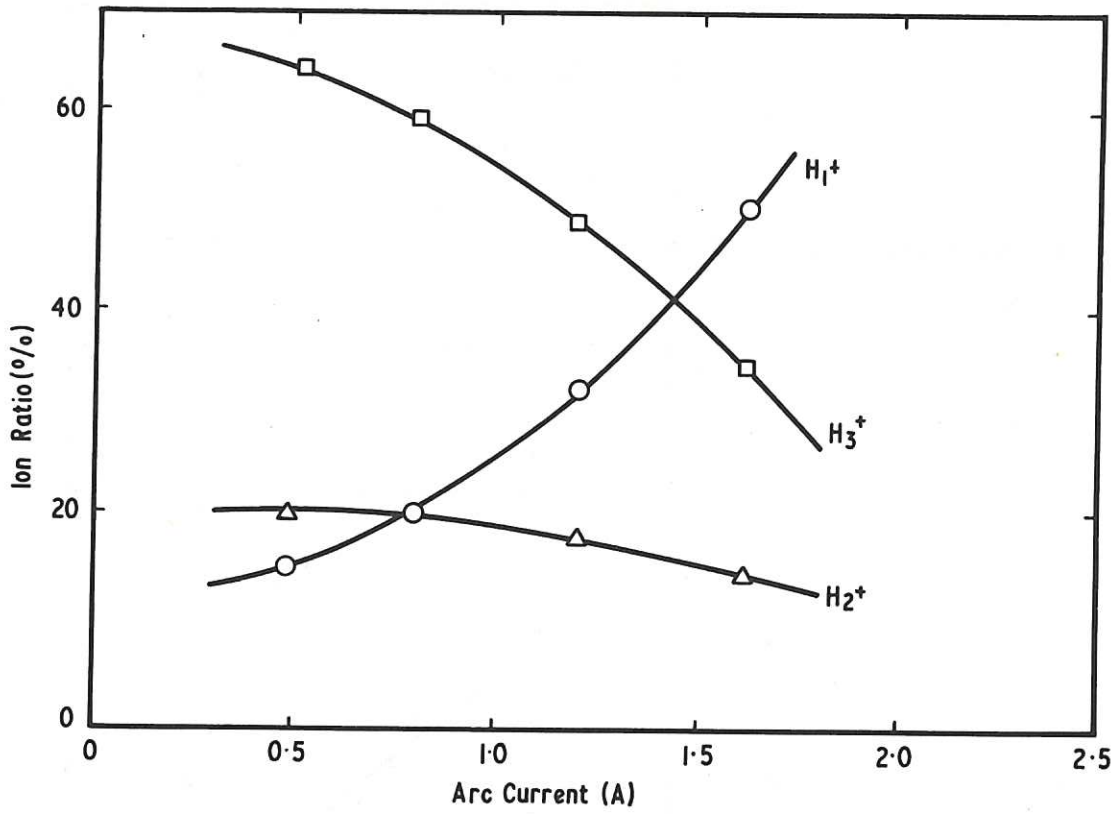

(a) Experimental results.

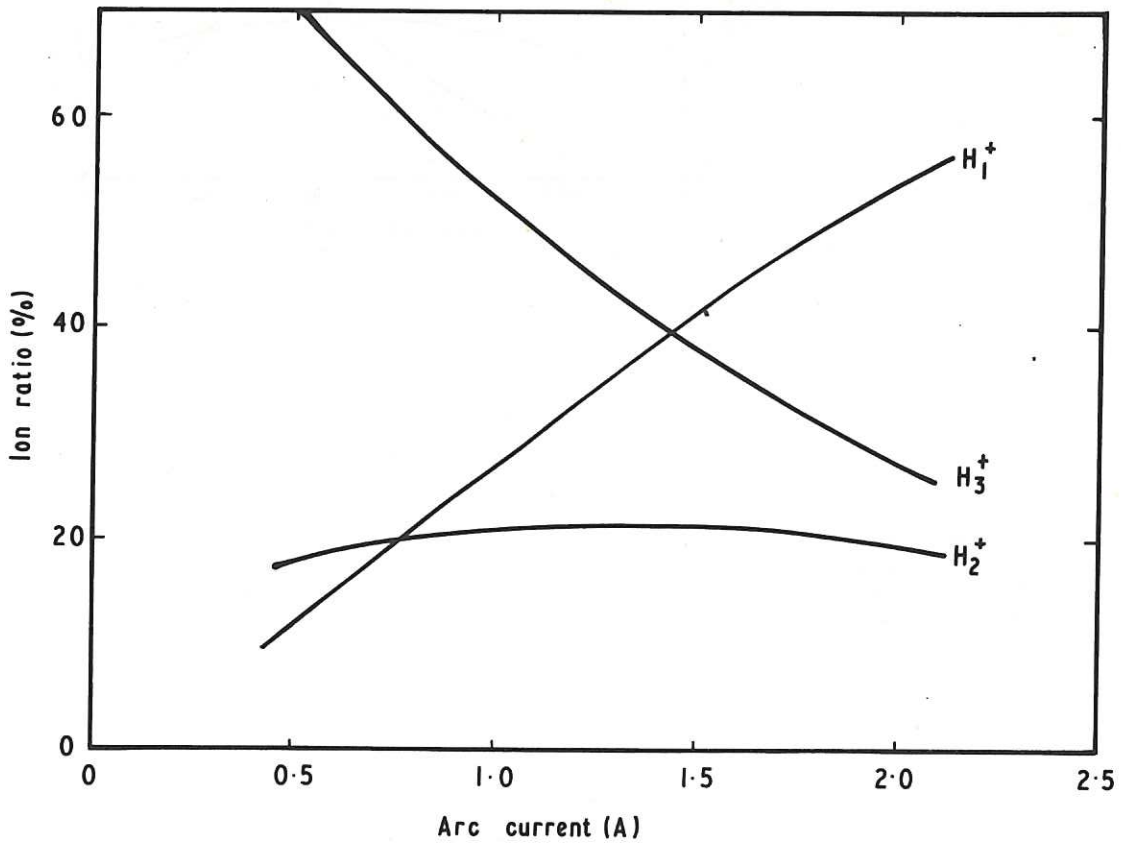

(b) Numerical results.

Fig.4 Ion ratio as a function of arc current at a gas pressure of 0.26 torr.

(a) Experimental results.

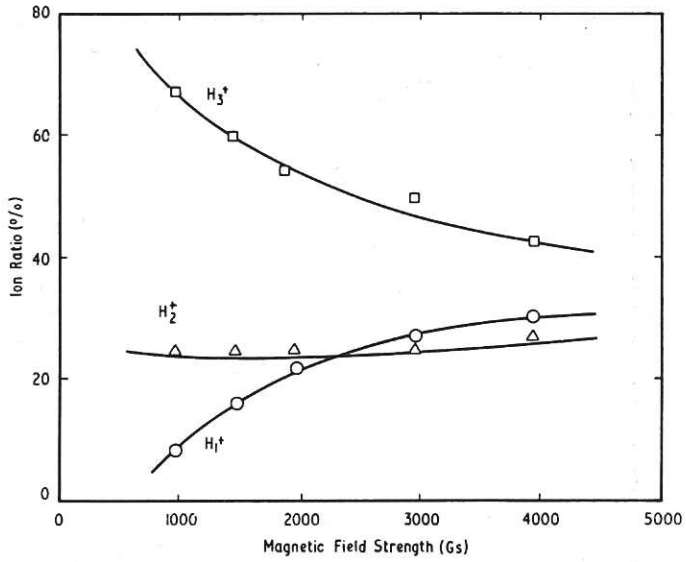

(b) Numerical results.

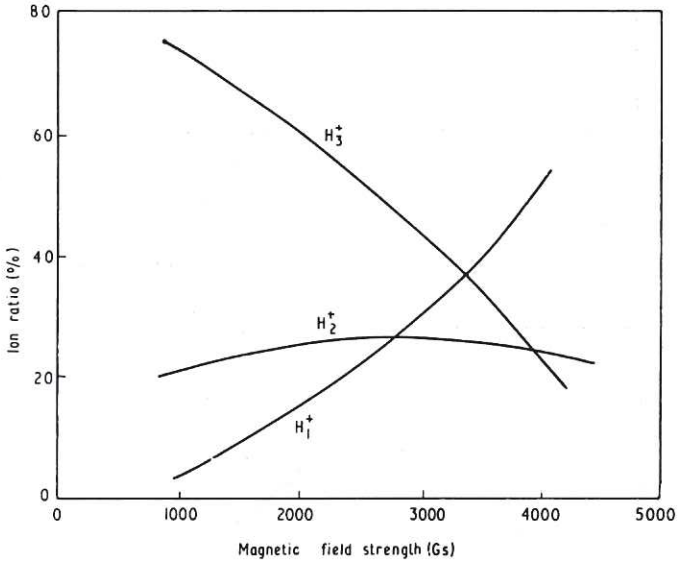

(c) Numerical results with the radius of the plasma column scaled as described in the text.

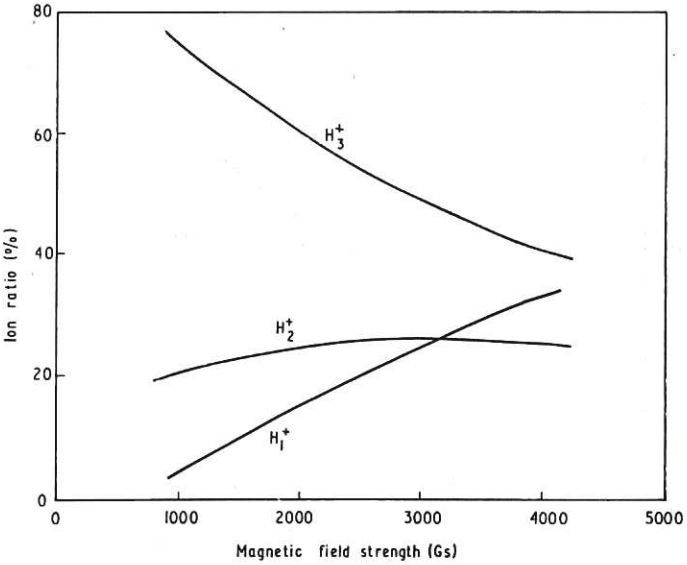

Fig.5 Ion ratio as a function of magnetic field strength at a gas pressure of 0.16 torr and an arc current of 0.5 A.

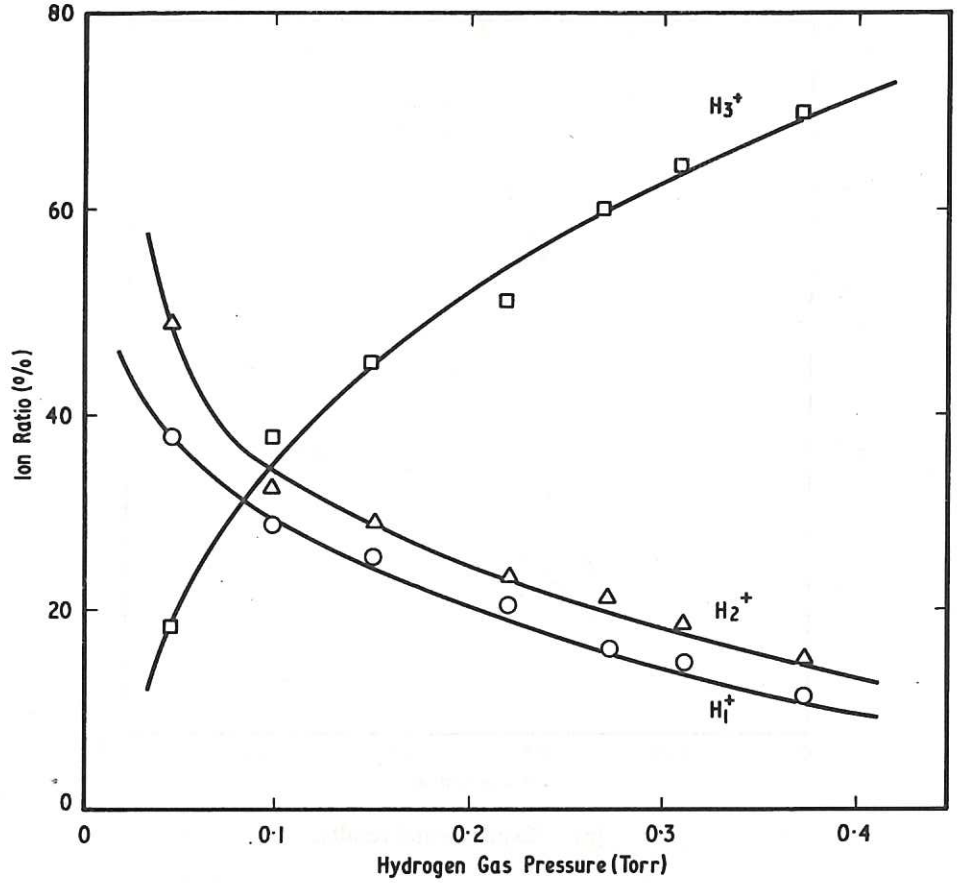

(a) Experimental results.

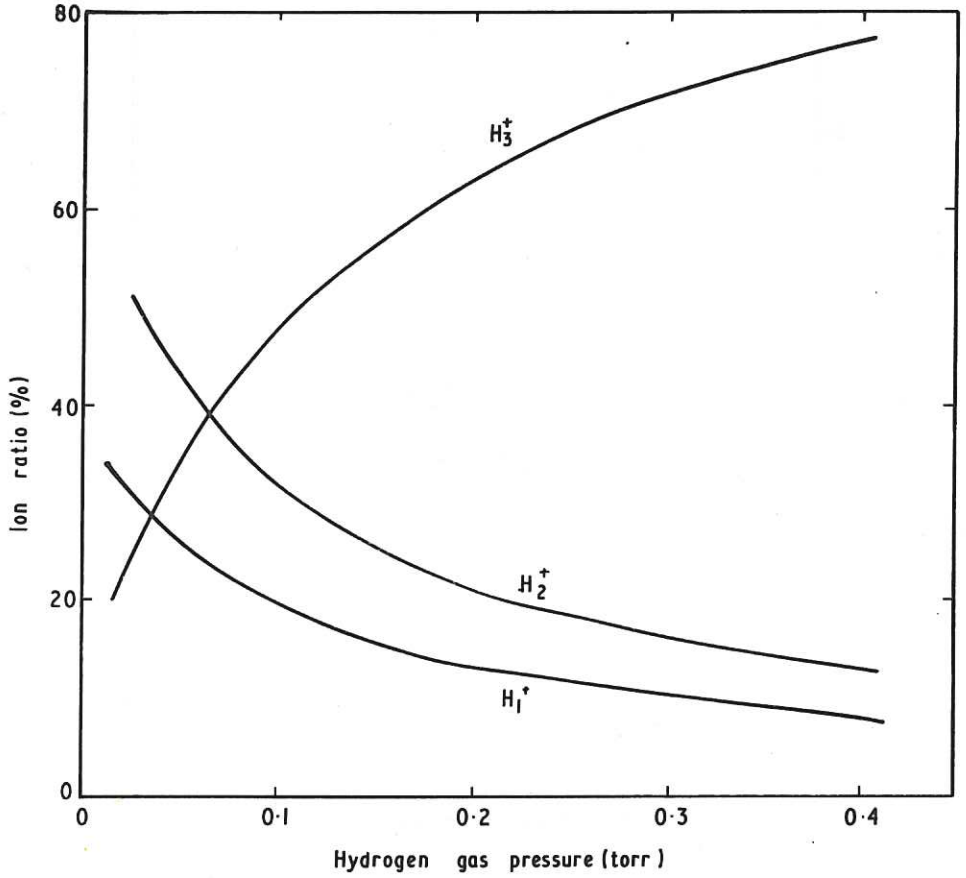

(b) Numerical results.

Fig.6 Ion ratio as a function of the gas pressure at an arc current of 0.5 A.

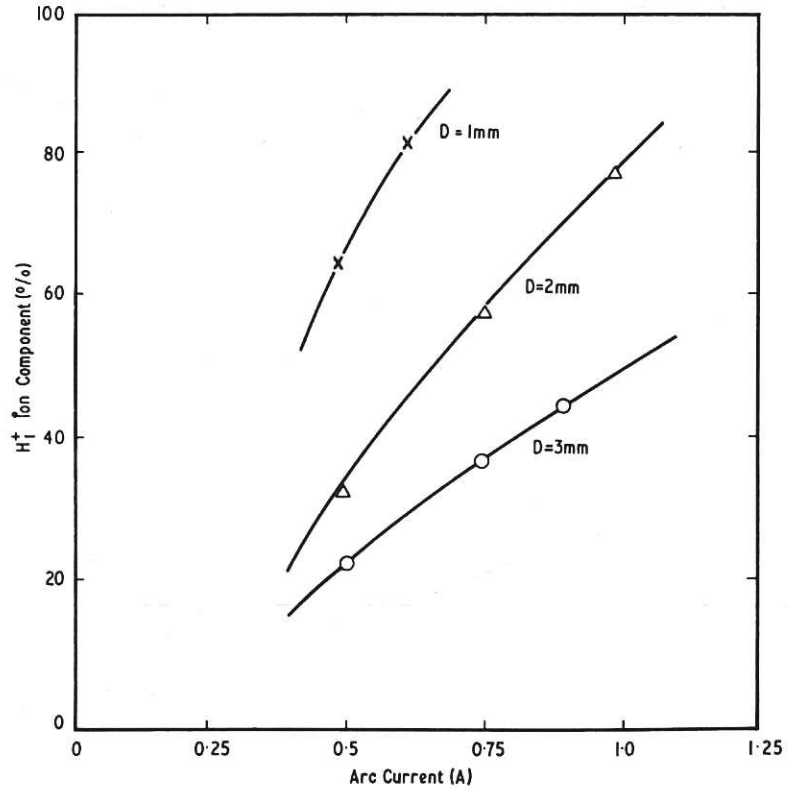

(a) Experimental results.

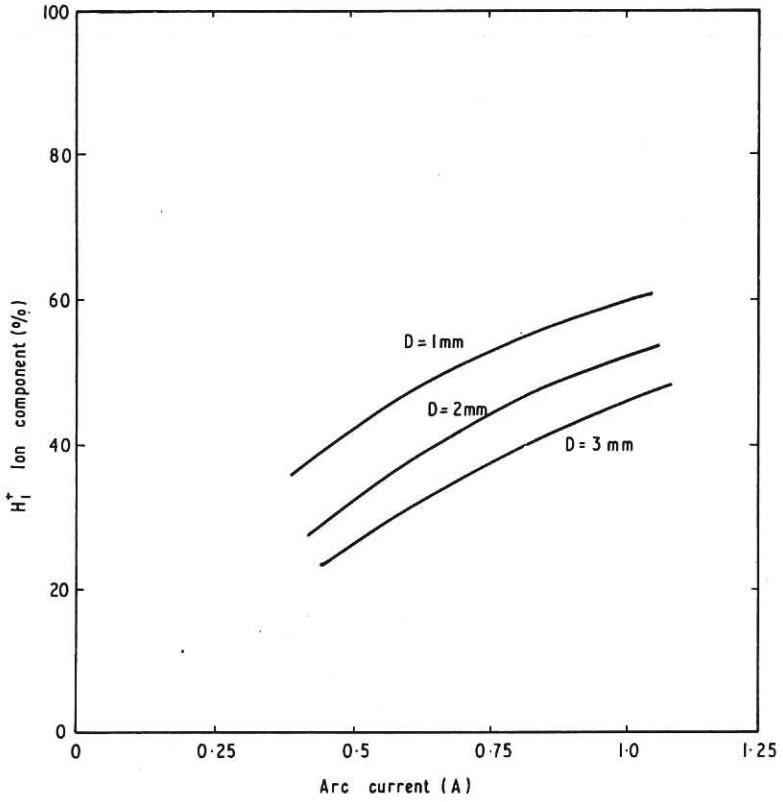

(b) Numerical results with $\tau \propto D$.

Fig.7 Proton fraction as a function of arc current, for different discharge lengths, D.

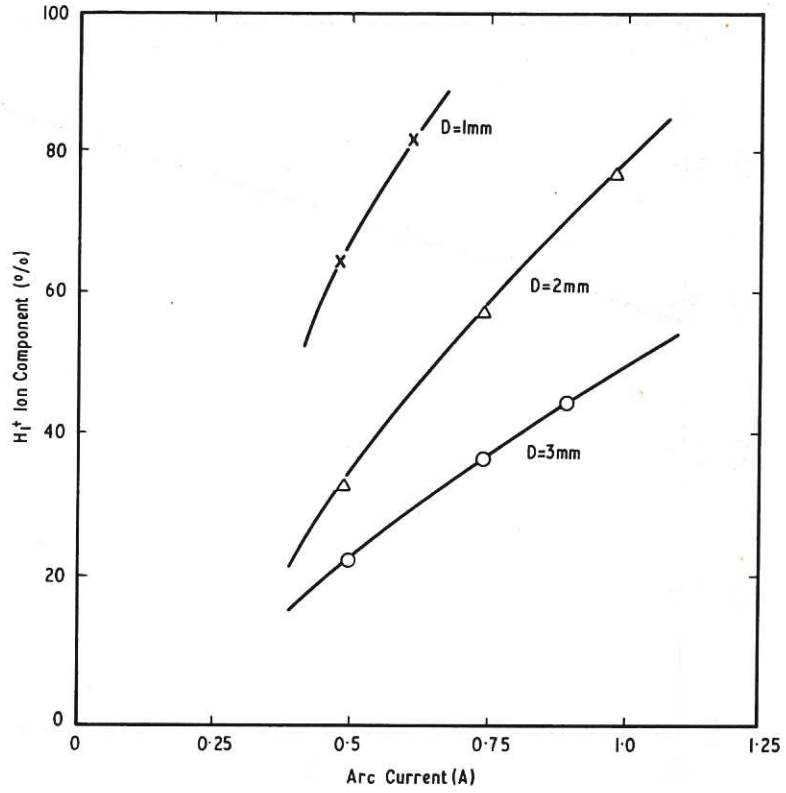

(a) Experimental results.

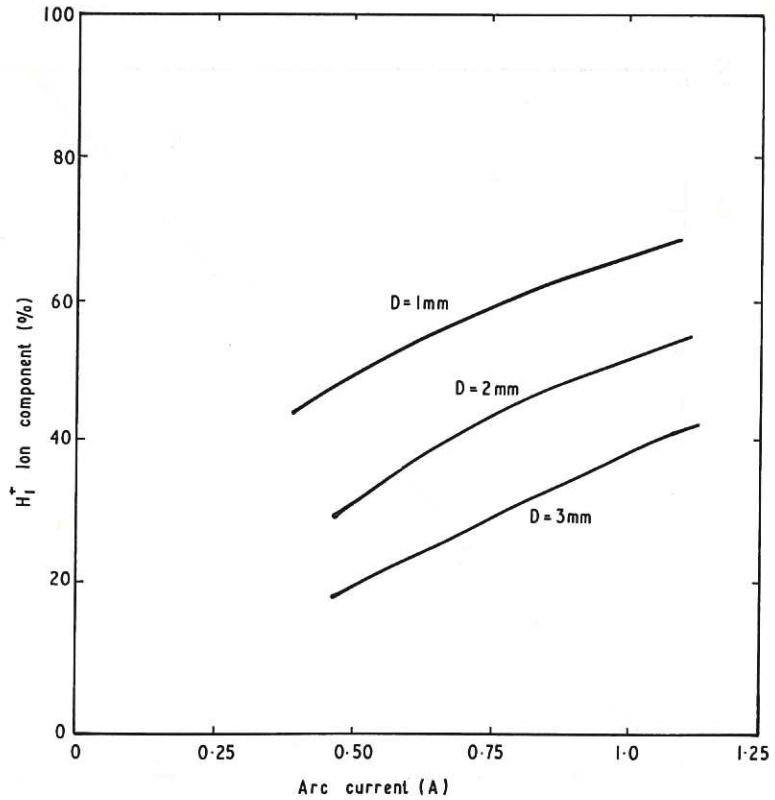

(b) Numerical results with $\tau \propto D^2$.

Fig.8 Proton fraction as a function of arc current for different discharge lengths, D.

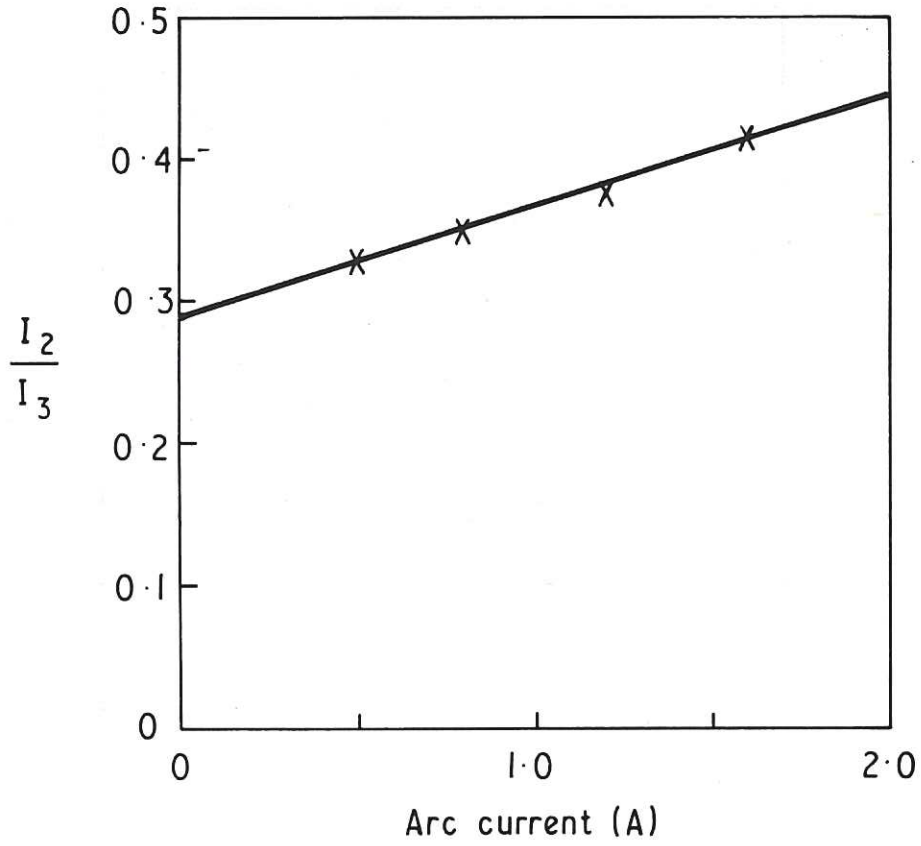

Fig.9 Variation of the ratio of currents of H_2^+ and H_3^+ (I_2/I_3) with arc current for the duoplasmatron. (Data from Fig.4)

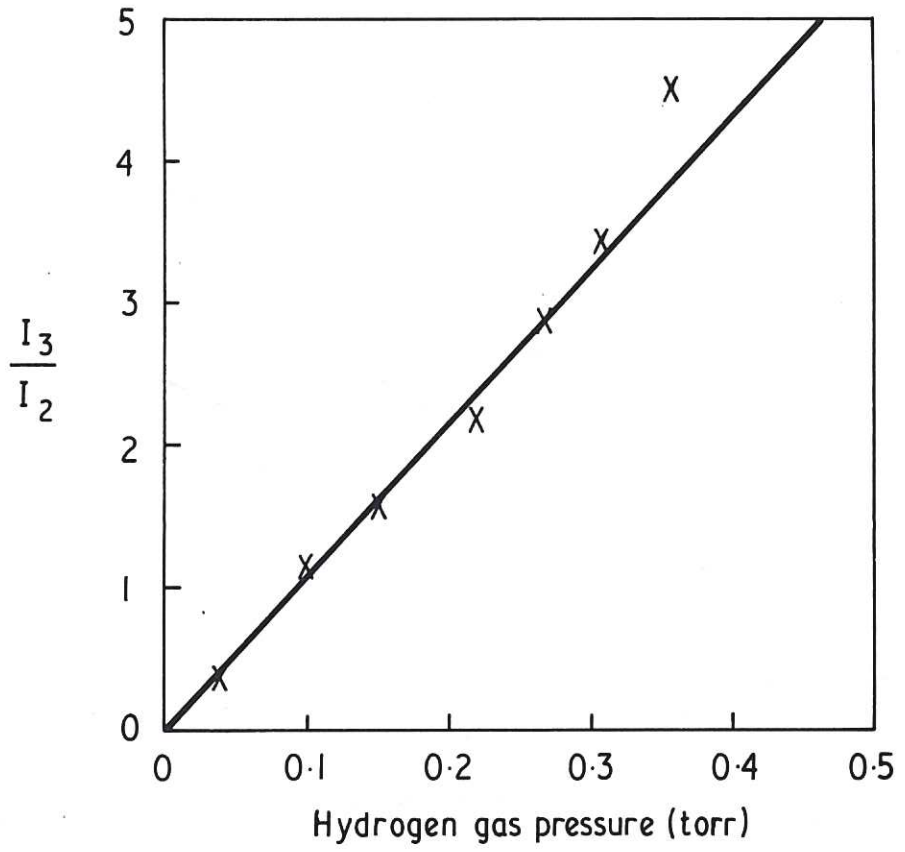

Fig.10 Variation of the ratio of currents of H_3^+ and H_2^+ (I_3/I_2) with gas pressure for the duoplasmatron. (Data from Fig.6)

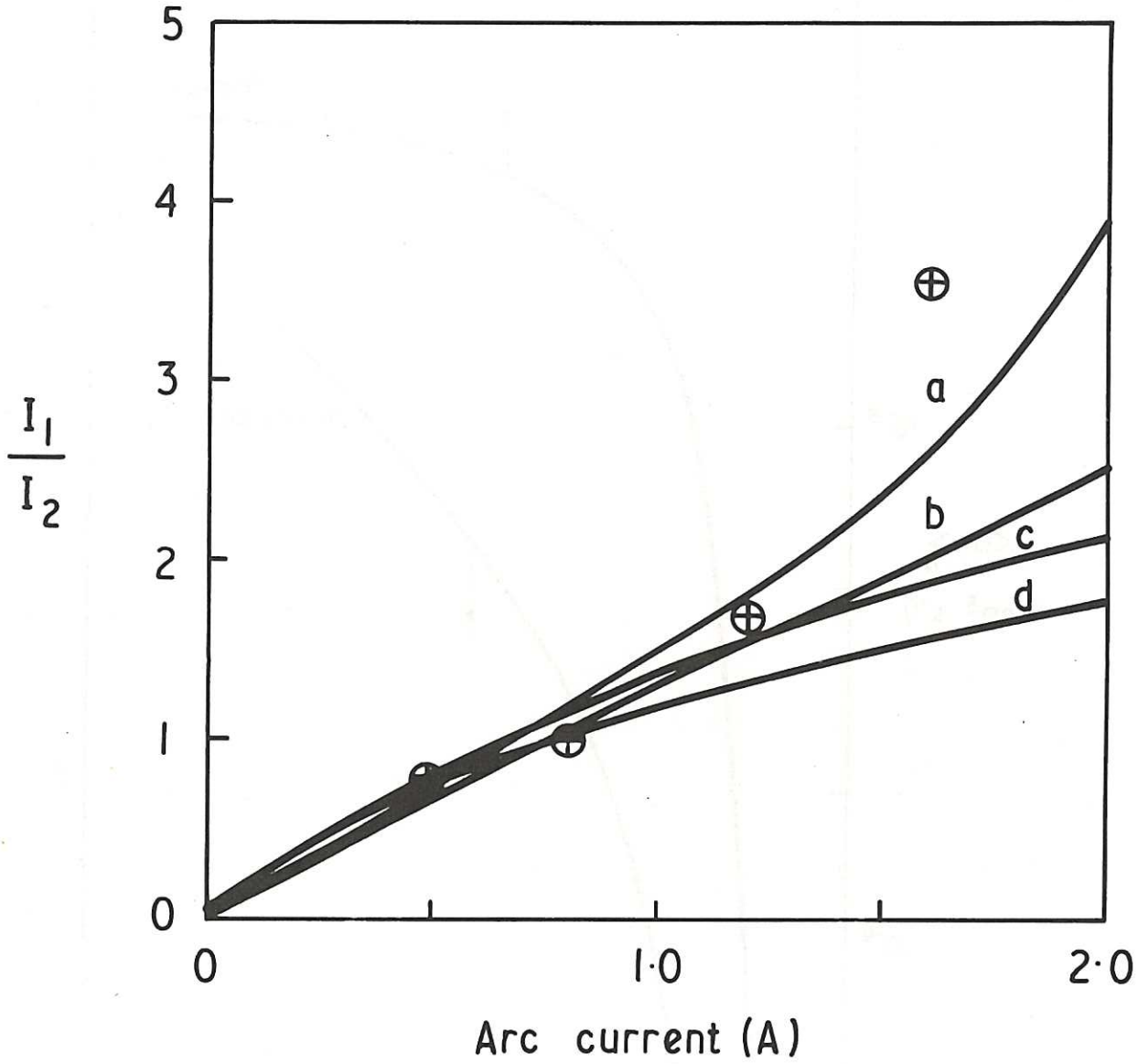

Fig.11 Variation of the ratio of currents of H^+ and H_2^+ (I_1/I_2) with arc current (I_e) for the duoplasmatron. Experimental points from Fig.4 – 0. Solid lines are computed for different values of $\alpha = \frac{2\langle\sigma v\rangle_{22}}{\langle\sigma v\rangle_{21}}$ and of $\beta = \frac{\gamma \tau_2}{T_1}$: (a) $\alpha = 6.0, \beta = 0.05$; (b) $\alpha = 4.0, \beta = 0.05$; (c) $\alpha = 2.0, \beta = 0.027$; (d) $\alpha = 0.4, \beta = 0.016$.

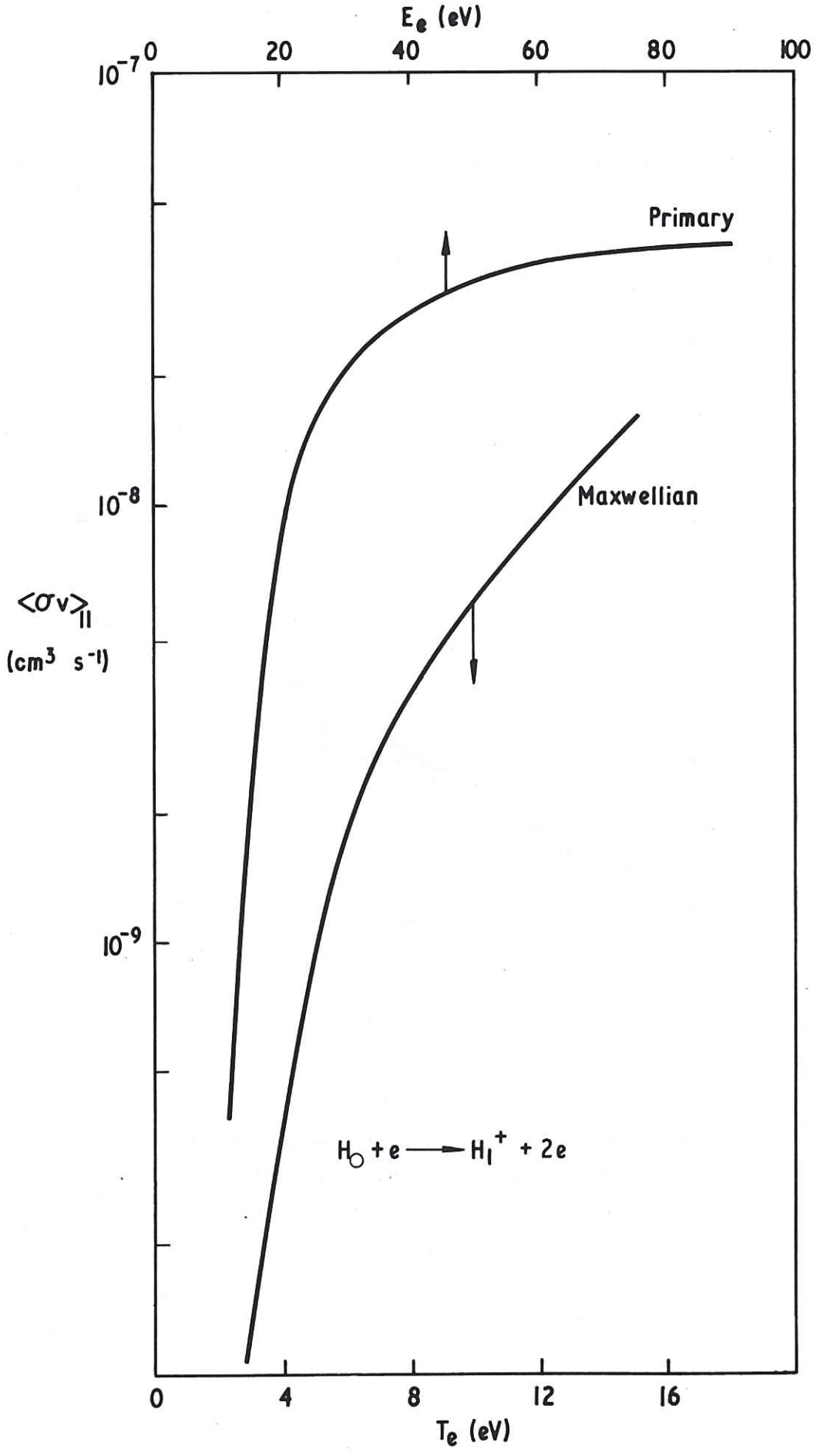

Fig.A1 Rate coefficients for ionisation of atomic hydrogen.

CLM-R 159

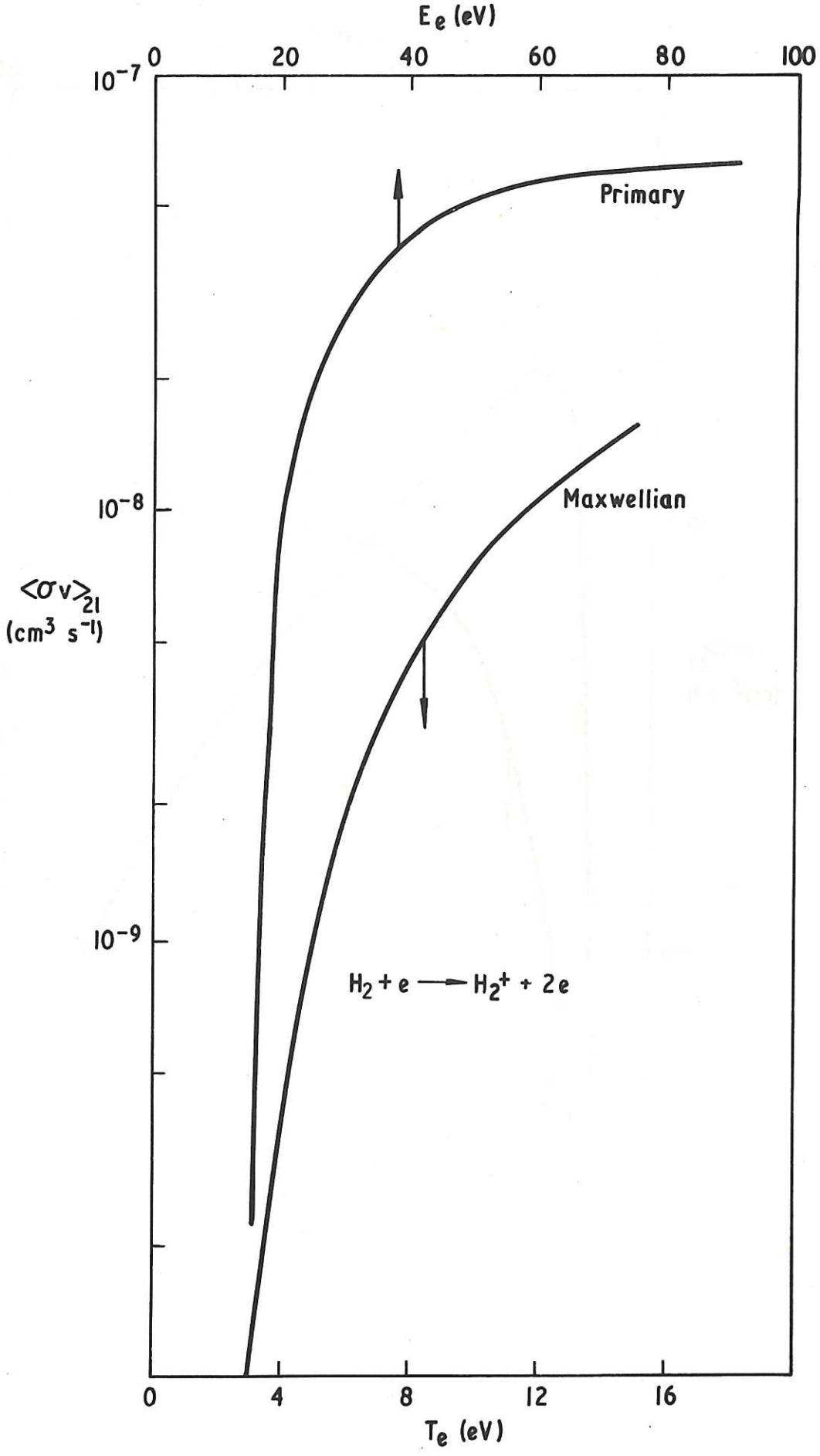

Fig.A2 Rate coefficients for ionisation of molecular hydrogen.

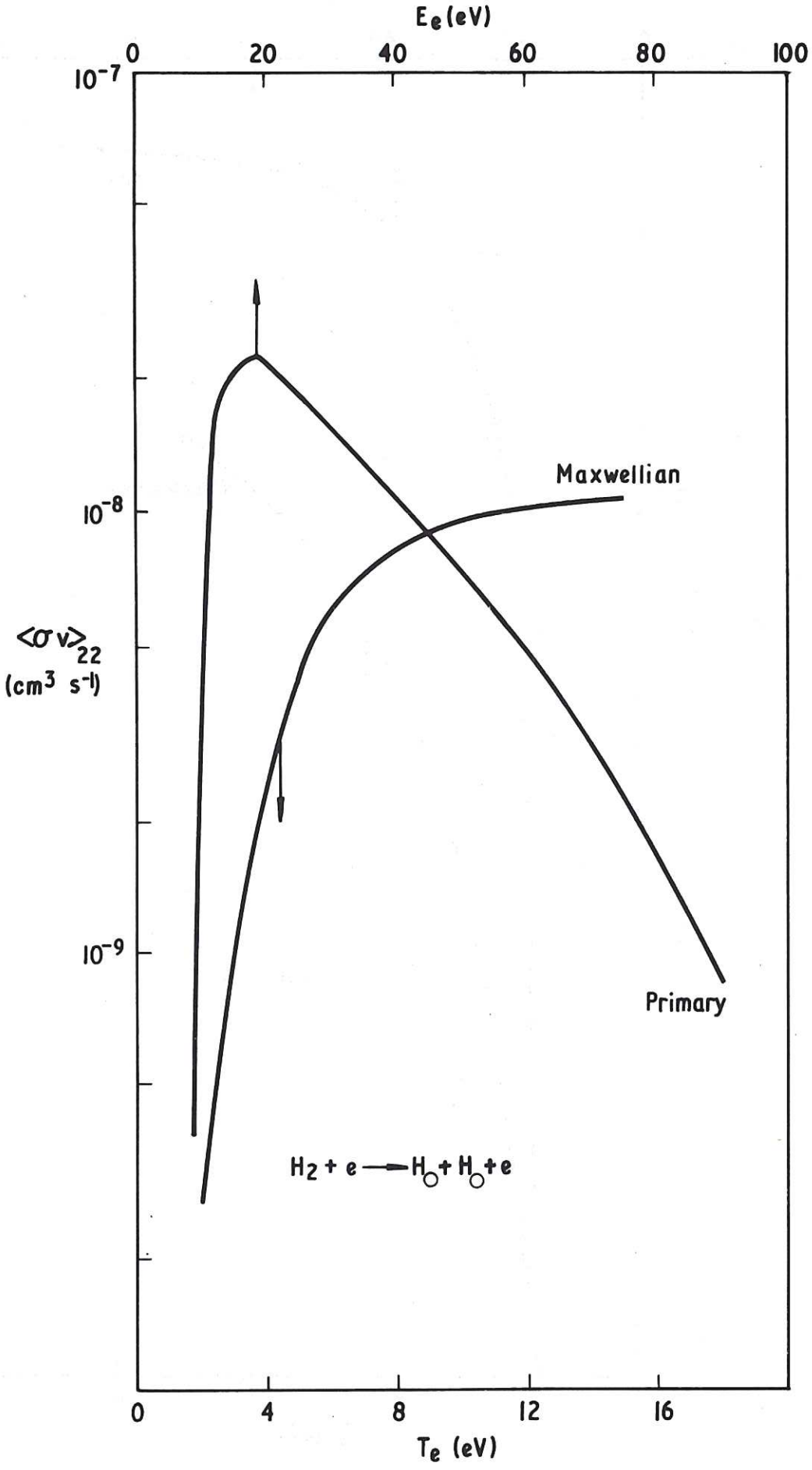

Fig.A3 Rate coefficients for dissociation of molecular hydrogen.

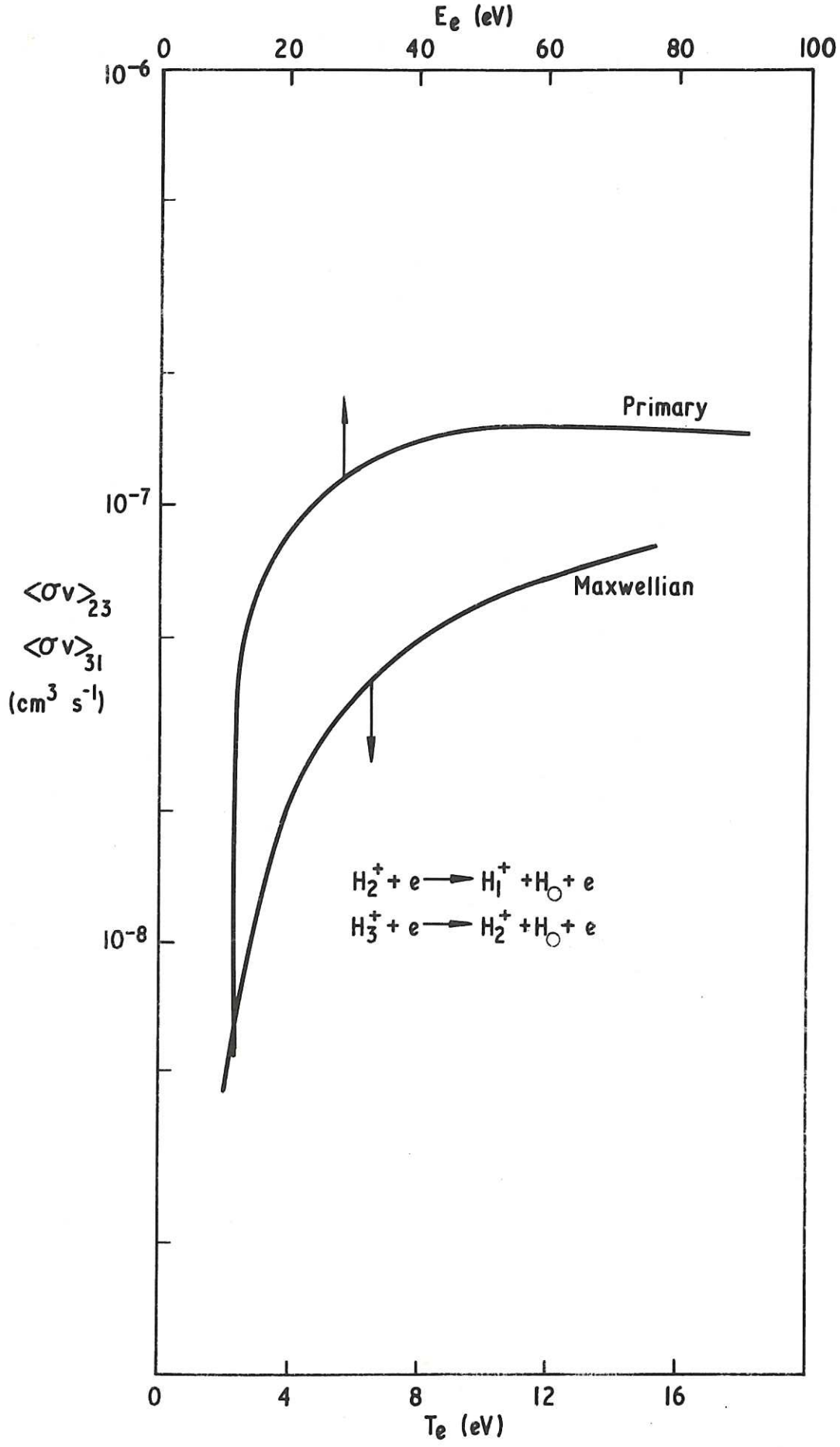

Fig. A4 Rate coefficients for dissociative excitation of H_2^+ ions, and for breakup of H_3^+ ions.

HER MAJESTY'S STATIONERY OFFICE

Government Bookshops

49 High Holborn, London WC1V 6HB
13a Castle Street, Edinburgh EH2 3AR
41 The Hayes, Cardiff CF1 1JW
Brazennose Street, Manchester M60 8AS
Wine Street, Bristol BS1 2BQ
258 Broad Street, Birmingham B1 2HE
80 Chichester Street, Belfast BT1 4JY

Government publications are also available through booksellers